

Disruption of *FOXF2* as a likely cause of absent uvula in a large Egyptian family

Rimante Seselgyte¹, Dale Bryant¹, Charalambos Demetriou¹, Miho Ishida¹, Emma Peskett¹, Nadjeda Moreno², Deborah Morrogh³, Debbie Sell⁴, Melissa Lees^{4,5}, Martin Farrall⁶, Gudrun E. Moore¹, Brian Sommerlad⁴, Erwin Pauws², Philip Stanier¹.

¹Genetics and Genomic Medicine, UCL GOS Institute of Child Health, London

²Developmental Biology and Cancer, UCL GOS Institute of Child Health, London

³NE Thames Regional Genetics Service Laboratory, Great Ormond Street Hospital NHS Trust, London

⁴North Thames Cleft Centre, St Andrew's Centre, Broomfield Hospital, Chelmsford, Essex, CM1 7ET and Great Ormond Street Hospital for Children NHS Foundation Trust, London

⁵Department of Clinical Genetics, Great Ormond Street Hospital NHS Trust, London

⁶Wellcome Trust Centre for Human Genetics, University of Oxford, Oxford.

Corresponding author: Philip Stanier, p.stanier@ucl.ac.uk +442079052867

Key words: Cleft palate, Craniofacial biology/genetics, gene expression, oral pathology, speech pathology, transcription factor(s).

Abstract

This study investigated the genetic basis of an unusual autosomal dominant phenotype characterized by familial absent uvula, with a short posterior border of the soft palate, abnormal tonsillar pillars and velopharyngeal insufficiency. Cytogenetic analysis and SNP-based linkage analysis were investigated in a 4-generation family with eight affected individuals. Whole exome sequencing data was overlaid and segregation analysis identified a single missense variant, p.Q433P in the *FOXF2* transcription factor, that fully segregated with the phenotype. This was found to be in linkage disequilibrium with a small 6p25.3 tandem duplication affecting *FOXC1* and *GMDS*. Notably, the copy number imbalances of this region are commonly associated with pathologies that are not present in this family. Bioinformatic predictions along with luciferase reporter studies of the *FOXF2* missense variant indicated a negative impact, affecting both protein stability and transcriptional activation. *Foxf2* is expressed in the posterior mouse palate and knockout animals develop an overt cleft palate. Since mice naturally lack the structural equivalent of the uvula, we demonstrated *FOXF2* expression in the developing human uvula. Decipher also records two individuals with hypoplastic or bifid uvulae with copy number variants affecting *FOXF2*. Nevertheless, given co-segregation with the 6p25.3 duplications, we cannot rule out a combined effect of these gains and the missense variant on *FOXF2* function, which may account for the rare palate phenotype observed.

Introduction

Clefts of the lip and/or the palate (CL/P) occur in around 1/700 births (Mossey et al, 2009). There is a wide phenotypic spectrum which may involve complete or incomplete bilateral or unilateral cleft lip, with or without cleft palate, as well as isolated cleft of the secondary palate. Isolated palate defects are etiologically distinct from cleft lip due to the contribution of different tissue lineages and distinct timing of various fusion events during development (Stanier and Moore, 2004, Harville et al., 2005, Mossey et al., 2009). Defects of the secondary palate range from complete cleft of the hard and soft palate, or affect the soft palate only. They also include submucous cleft palate (SMCP), where the palatal shelves have fused and the oral mucosa is intact, while a bony notch in the posterior hard palate, translucency in the soft palate (reflecting abnormally inserted levator palati muscles), and a bifid uvula are characteristic features (Calnan, 1954, Pauws et al., 2009). When muscle malposition occurs in the absence of the triad of overt signs, it is called occult SMCP (Kaplan, 1975). A spectrum of abnormality as well as the functional impact varies between classical and occult SMCP (Sommerlad et al., 2004). Consequences can be very mild, remaining undiagnosed (Meskin et al., 1964) or identified incidentally (e.g. during adenoidectomy). In other cases, similar problems to an overt cleft are experienced (Swanson et al., 2017), including significant feeding difficulties with nasal regurgitation, conductive hearing loss due to otitis media and poor speech (de Blacam et al., 2018). In patients with SMCP, speech may be characterized by hypernasality, audible nasal emission and the cleft characteristics of passive and nonoral articulation errors, which significantly compromise intelligibility (Sell

et al., 1999). This results from effects on the anatomy of the velopharynx. The velopharyngeal mechanism consists of a muscular valve that extends from the posterior surface of the hard palate to the posterior pharynx and includes the soft palate and lateral and posterior pharyngeal walls. The velopharyngeal mechanism creates a tight seal between the velum and pharyngeal walls to separate the oral and nasal cavities during speech and swallowing (Perry, 2011, Mardini et al., 2016). Failure of the velopharyngeal sphincter to close may either be an anatomical or a physiological limitation depending on the severity of the palate defect, leading to velopharyngeal insufficiency (VPI).

In this study we have investigated a highly unusual, familial palate defect, associated with the clinical presentation of VPI. Affected individuals in an autosomal dominant family present with no uvula, a short posterior border of the soft palate and apparent absence of the anterior tonsillar pillars with rudimentary posterior pillars (Figure 1). To investigate the genetic basis of this condition, we report our genetic studies, which identify small 6p25.3 duplications co-segregating with a missense variant in *FOXF2* as the likely cause of this condition.

Materials and Methods

Patients and clinical evaluation

The pedigree consists of a four-generation Egyptian family with autosomal dominant hypernasality and absent uvula with a short posterior border of the soft palate and abnormal tonsillar pillars (Figure 1). Specialist speech pathology assessment was undertaken for IV.5. Perceptual examination revealed mild hypernasality with cleft speech characteristics (Sell et al., 1999). A diagnosis of VPI was based on lateral videofluoroscopy which showed a thin velum with poor lift. Also, there were small adenoids above and at the plane of attempted closure with some slight movement of the posterior pharyngeal wall. The medical history included feeding difficulties with nasal regurgitation after birth. No other medical issues were recorded. Visual inspection and digital recording of oral pathology for IV.5 and other family members was also conducted.

Detailed materials and methods are included in the Appendix.

Results

An Egyptian boy (IV.5) presented with a clinical history of occasional nasal regurgitation while breastfeeding in infancy, followed by speech and language delay and hypernasality. On examination at 3 years the patient's uvula was absent and the posterior border of the soft palate appeared short, the anterior tonsillar pillar was also absent while the posterior pillar was rudimentary (Figure 1A). There was poor velar movement. There were no obvious syndromic features. The family history revealed seven other individuals also with no uvula, along with a tight posterior border of the velum and pillar structure (Figure 1B). All affected family members had mild hyper nasal speech.

Genome-wide cytogenomic microarray analysis of the proband excluded a deletion at 22q11.2 but indicated the presence of two duplications on 6p25.3 (Appendix Figure 1). A small gain (227,481bp) overlapped only with a single predicted but uncharacterized, noncoding mRNA (LOC285768) and a 480,000 bp gain, encompassing *FOXC1* and the 5' exons of *GMDS*. A qPCR assay for *FOXC1* confirmed the presence of the CNV and demonstrated inheritance from the father and his paternal grandmother, who both had palates of similar appearance and had mild hypernasality. The variant was not present in the proband's mother.

Linkage analysis

SNP based genotyping was performed on 11 individuals from the family (Figure 1B). III.5, III.7 and III.8 were unavailable at this time. Quality control analysis indicated no inconsistencies between the "inferred from X-chromosome genotype data" and the

recorded sex. The overall genotype missingness rate (a high rate of missing genotype calls can imply poor quality genotyping) was very low (>0.003157). The genome average identity by descent data was consistent with the communicated family structure. Following QC, a set of 5,497 informative autosomal SNPs located at approximately 0.5 cM spacing were selected for parametric linkage analysis. These SNPs captured 89% (SE 4.2%) of the theoretical maximal linkage information in the family. Ten regions fully segregated with the phenotype, reaching the maximum LOD score of 1.5. One small region narrowly failed to reach this score (Appendix Figure 2). Collectively, these intervals contained approximately 760 RefSeq genes and spanned a little over 100 million bases. The likely causal gene was expected to segregate with one of these intervals.

Exome sequencing

Exome sequencing was performed on two affected (IV.5 and III.6) individuals and one unaffected female (III.2) who had 3 unaffected children (Figure 1B). Sequencing data was analyzed as described in the Appendix. Twenty-one candidate variants were present in both affected individuals but not in the unaffected individual. Eleven of these were excluded following alignment to the linkage data. The ten remaining variants were therefore considered as candidates. Each variant was validated using Sanger sequencing. Details of each candidate variant (*PLB1*; *FOXF2*; *SNX10*; *PLIN2*; *IGDCC3*; *THSD4*; *SEMA7A*; *SCAPER*; *SH2D7* and *IL16*) are presented in Appendix Table 1 and bioinformatics analysis in Appendix Table 2. Three additional family members (III.5; III.7 and III.8) (Figure 1B) were later recruited and Sanger sequencing to investigate

segregation (along with III.6) for each of the 10 variants by. Only the c.1298A>C (p.Q433P) variant in *FOXF2* fully segregated with the phenotype and was therefore considered the most likely pathogenic variant (Appendix Figure 3). Incorporating the new individual's variant genotypes from each candidate loci as additional SNPs into the linkage analysis, the LOD score at 6p25.3 increased to 1.9. While at each of the other loci, LOD scores reduced to between -0.4 and 1.4.

The *FOXF2* c.1298A>C variant has been reported twice in two heterozygous European individuals of unknown phenotype in gnomAD and ExAC databases. No other information is reported about these individuals. Two further missense substitutions are also reported at the same position, p.Q433H (Latino) and p.Q433G (East Asian), at 1/246,272 alleles. In terms of amino acid conservation, the glutamine residue is well conserved across species, excluding chicken and lamprey (Figure 2). Interestingly, the *FOXF2* variant is very close to and in linkage disequilibrium with the 6p25.3 tandem duplication identified by the cytogenetic analysis.

Analysis of *FOXF2* in individuals with non-syndromic CP and SMCP

To investigate whether *FOXF2* pathogenic variants might underlie more common forms of cleft palate, a cohort of patients with non-syndromic CP (240) or SMCP (72) were sequenced. Variants identified are listed in Appendix Table 3 and depicted in Figure 2 and Appendix Figure 4. Only two rare/unique missense variants were identified (Appendix Figure 4A, B), neither predicted damaging by bioinformatics analysis (Appendix Table 3). Two common missense variants were also identified (Appendix Figure 4C, D): at 6:1390576, c.394G>A (p.A132T) was in 170/19,842 alleles in Asian

heterozygotes in the gnomAD database, while at 6:1390882, c.700C>A (p.P234T), was present in the African population in 182 heterozygotes and 3 homozygotes in 16,934 alleles and 28/30,890 Latino heterozygotes. Since these variants were described as benign (Appendix Table 3), they were not studied further. No variants of interest were identified in the coding sequence of *FOXF2* in exome sequencing data generated from ~30 multiplex, non-syndromic CL with or without CP (NSCLP) families from previous genetic studies.

Effect on transcriptional activation

Since the p.Q433P variant is located in the previously described Activation Domain (AD1) (Hellqvist et al., 1998) (Figure 2), we investigated the effect of the point mutation on *FOXF2* transcriptional activity using transient luciferase reporter assays. Wildtype and p.Q433P constructs were co-transfected into HeLa cells along with a *FOXF2* luciferase reporter plasmid, which contained four consecutive *FOXF2* binding sites (Hellqvist et al., 1998). Both WT and p.Q433P constructs produced significant activation compared to empty vector, while the pathogenic variant caused a significant 1.5 fold increase in activation compared to the wildtype sequence (Figure 3A). Interestingly, whilst a 0.3 fold reduction in quantitative expression difference was observed between the WT and p.Q433P constructs (Figure 3B), a dramatic and reproducible 11 fold increase in the quantity of the *FOXF2*-Q433P protein compared to wildtype was detected by Western blotting (Figure 3C). Both constructs were sequenced in their entirety and plasmid DNA was accurately measured using several methods to ensure even loading. A similar result was reproducibly obtained following transfection into

HepG2 cells and several independent clones gave similar results (data not shown). We also calculated luciferase activity normalized to protein levels (Figure 3D), since it is not known how the mutation might affect the translation of endogenous FOXF2 protein levels *in vivo* during embryonic development. This analysis shows effectively an 88% loss of activation relative to the amount of FOXF2 protein present.

Based on the findings of Xu et al, (2016) who reported upregulation of *Fgf18* and downregulation of *Shox2* expression in *Foxf2* knockout mice, we investigated the effect of overexpressing FOXF2 on both of these genes in HeLa cells (Xu et al., 2016). Although no effect was detected for SHOX2, FGF18 was found to be significantly upregulated when overexpressing the FOXF2-Q433P variant in comparison to the WT sequence (Figure 3E, F and Appendix Figure 5).

Expression of FOXF2 in craniofacial tissues

Foxf2 has been previously established as required for normal palate closure in the mouse (Wang et al., 2003) and its expression in the developing orofacial region is restricted to the posterior palate and tongue (Nik et al., 2016, Xu et al., 2016). However, since mice lack a structure equivalent to the uvula, we investigated FOXF2 expression in coronal sections of human embryos around the time of palatogenesis using *in situ* hybridisation (Figure 4). Similar to the mouse, FOXF2 is expressed in the human embryonic mesenchyme of the oral cavity and tongue. This is particularly notable in the posterior palatal shelves before fusion at Carnegie stages 22-23, decreasing significantly in the fused palate found at late 8th post conception week. Expression was still seen in the most posterior region of the L8pcw embryo where the palatal shelves

had not yet fused and extended to the oral epithelia in addition to the mesenchyme. This region is equivalent to the presumptive uvula.

Discussion

In this study, we have identified a putative dominantly acting missense mutation in the activation domain of *FOXF2*, which fully segregates in a multigeneration family that includes eight affected individuals. All present with absent uvula, short anterior border of the soft palate and abnormal pillars of the fauces, a rare disorder of palate development. In the mouse, *Foxf2* is expressed in the posterior region of the secondary palate and homozygous loss of function results in a complete cleft of the secondary palate (Wang et al., 2003). Although mice naturally lack an uvula, we show here that *FOXF2* is also expressed in the posterior human palate during development, including the rudimentary uvula.

The *FOXF2* variant was identified using a combination of linkage analysis and exome sequencing followed by further segregation analysis. Cytogenetic analyses performed during the preliminary investigation revealed two small duplicated regions in 6p25.3, which flank *FOXF2* and also segregated with the phenotype. The larger of these overlaps with two known genes *FOXC1* and *GMDS*. Considering this CNV as a potential cause for the absent uvula phenotype, CNVs of this interval as well as dominant mutations in *FOXC1* are reported to cause glaucoma and/or Axenfeld-Rieger syndrome, which is characterized by Dandy Walker malformation and cerebellar hypoplasia (Gould et al., 1997, Aldinger et al., 2009), sometimes including micro- or hypodontia. Duplications of this interval have also been reported, notably in a large

pedigree characterized by glaucoma and iris hypoplasia (Lehmann et al., 2000). However, in the Egyptian family, none of the individuals with the duplication display any obvious eye or brain malformation, suggesting that in this respect, the CNV is likely benign. Notably, the *FOXF2* variant lies only ~200kb distant to the proximal duplication. Decipher lists 52 individuals who have chromosomal gains or losses encompassing this region (Firth et al., 2009). Whilst the majority of these have eye anomalies, one individual with a 1.7Mb duplication including *FOXF2* was reported to have a bifid uvula as well as hyperparathyroidism (Appendix Figure 1). This CNV was inherited from an unaffected father. Another individual with a small heterozygous deletion including only the *FOXQ1* and *FOXF2* loci (Appendix Figure 1), was reported to have a hypoplastic uvula and dysarthria, among other pathologies. This individual also had a *de novo* chromosome 5 duplication and a chromosome 2 duplication, while the 6p loss was implied benign being inherited from his apparently unaffected father. Nevertheless, this rare description in Decipher and the precise location is striking.

A possible explanation for how a gain could impact nearby gene expression during palate development is via disruption of a local topologically associated domain (TAD) (Lupianez et al., 2016; Thieme and Ludwig, 2017). TADs, which define boundary regions where DNA sequences such as promoter-enhancer contacts occur, are often marked by CTCF binding sites. Although cells relevant to the fetal uvula development have not yet been investigated, numerous CTCF binding sites conserved across multiple cell lines have been identified (<http://genome.ucsc.edu/>). These include at least one within the CNV immediately distal to *FOXF2*, which by impacting a relevant TAD, could compound with the effect of the missense mutation. In the context of the family

reported here, given the proximity and shared segregation, it is therefore difficult to rule out a role for both the CNV and the missense variant in the causality of the uvula phenotype.

Mammals have two *FoxF* genes, *FoxF1* and *FoxF2* (previously *FREAC-1* and *FREAC-2*) in man and *Lun* in mouse (Carlsson and Mahlapuu, 2002, Clevidence et al., 1994, Pierrou et al., 1994, Miura et al., 1998). The expression pattern of *Foxf2* includes the mesenchyme of the oral cavity and the tongue, but is also present in fetal and adult lung, the placenta, and low levels in the prostate, small intestine, colon and fetal brain. It is, however, strongly expressed in the posterior secondary palate immediately prior to and during palatal shelf fusion and *Foxf2*^{-/-} mutants die at birth with a cleft of the secondary palate (Wang et al., 2003, Xu et al., 2016, Nik et al., 2016). *Foxf1* is more widely expressed in early embryogenesis and knockout mice die by mid-gestation caused by vasculature abnormalities (Ormestad et al., 2004).

FOXF2 is well characterized as a transcription factor, consisting of a DNA binding domain and two transcriptional activation domains (AD1 and AD2) (Blixt et al., 1998). *Foxf2* is a downstream target of an epithelia-mesenchymal interaction in the developing palate that involves FGF signaling in the mesenchyme, which in turn activates *Shh* expression in the epithelium (Nik et al., 2016, Xu et al., 2016). This pathway is also linked to TGFβ signaling, which explains consequential mesenchymal hypoplasia and cleft palate in mutants.

The p.Q433P variant in *FOXF2* is located within AD1 (Hellqvist et al., 1998) and was predicted to be damaging by bioinformatics analysis. We therefore investigated

transcriptional activity of wildtype and p.Q433P FOXF2 proteins using a luciferase reporter assay in both HeLa and HepG2 cells as previously described (Hellqvist et al., 1998). Surprisingly we found that the variant resulted in significant up-regulation of FOXF2 protein. Since transcript levels were constant, this might be explained either by more efficient protein translation, or by increased protein stability. Alternatively high levels of overexpressed wildtype protein might be problematic for the cells and therefore translation actively restricted or degraded. None of these possibilities were investigated further here, but would be interesting to pursue in future work. In the context of increased protein levels, the reporter analysis showed a net increase in luciferase activity compared to wildtype. However, expression levels are driven by the constitutive CMV promoter in the construct and thus is not designed to replicate regulation of this locus *in vivo*. By expressing the activity as a factor of the protein level, the variant resulted in a considerable loss of activity, which might more truly reflect the result of mutation in the activation domain. It was therefore interesting to note a comparative increase in *FGF18* expression in HeLa cells overexpressing mutant compared to WT FOXF2, which was the same general trend observed for mice lacking *Foxf2* (Nik et al., 2016). Despite these cells not being a biologically relevant cell type for native FOXF2 expression, overall, a similar effect was replicated.

Further evidence for a role of FOXF2 in orofacial clefts was reported by Bu et al., (2015) who identified an association between two intronic SNPs and their concordance with NSCL/P in an Asian population. Therefore, in an attempt to further investigate FOXF2, we chose to sequence a cohort of CP and SMCP patients. In the absence of other cases with an absent uvular phenotype, these patients were considered the most

likely to be on the same phenotypic spectrum, especially since SMCP is often associated with bifid uvula. However, no likely causal mutations were identified. Instead, only two rare but 'benign' missense variants from the N-terminal portion of the protein were detected. It is possible that patients with NSCLP might have represented a better cohort, as suggested by the association data (Bu et al., 2015), but this remains to be tested. Furthermore, non-coding regulatory elements should not be ignored (Seto-Salvia and Stanier, 2014, Thieme and Ludwig, 2017). Nevertheless, our data potentially reflects the rarity of the absent uvula phenotype and lack of phenotype-genotype overlap with other palate anomalies.

In conclusion, whilst *FOXF2* is strongly implicated for absent uvula, the presence of nearby chromosomal duplications are confounding factors that may also contribute, potentially in combination with the *FOXF2* variant, by affecting transcriptional regulation of this or nearby genes. Further detailed analysis will be required to investigate the precise mechanisms involved. It would therefore be helpful to identify further families with a similar phenotype who also have mutations in this gene or nearby CNVs in order to further dissect their individual roles.

Acknowledgments

We would like to thank the Egyptian family for providing biological samples and clinical information. We are also grateful to Peter Carlsson for discussion and advice regarding the transient transfection experiments. A studentship to RS and the project was funded by CLEFT- Bridging the Gap. The human embryonic and fetal material was provided by the Joint MRC/Wellcome Trust (Grant #099175/Z/12/Z) Human Developmental Biology Resource (www.hdbr.org) and we thank Dianne Gerrelli for assistance with the *in situ* hybridization studies. PS is supported by Great Ormond Street Hospital Children's Charity. This research was also supported by the NIHR Great Ormond Street Hospital Biomedical Research Centre. The views expressed are those of the author(s) and not necessarily those of the NHS, the NIHR or the Department of Health. The authors declare no conflicts of interest.

References

- Aldinger KA, Lehmann OJ, Hudgins L, Chizhikov VV, Bassuk AG, Ades LC, Krantz ID, Dobyns WB, Millen KJ. 2009. FOXC1 is required for normal cerebellar development and is a major contributor to chromosome 6p25.3 Dandy-Walker malformation. *Nat Genet.* 41(9):1037-1042.
- Blixt A, Mahlapuu M, Bjursell C, Darnfors C, Johannesson T, Enerback S, Carlsson P. 1998. The two-exon gene of the human forkhead transcription factor FREAC-2 (FKHL6) is located at 6p25.3. *Genomics.* 53(3):387-390.
- Bryant D, Liu Y, Datta S, Hariri, H, Seda M, Anderson G, Peskett E, Demetriou C, Sousa S, Clayton P, et al. 2018. SNX14 mutations affect endoplasmic reticulum associated neutral lipid metabolism in autosomal recessive spinocerebellar ataxia 20. *Hum Mol Genet.* 27(11):1927-1940.
- Bu I, Chen Q, Wang H, Zhang T, Hetmanski JB, Schwender H, Parker M, Chou YH, Yeow V, Chong SS, et al. 2015. Novel evidence of association with nonsyndromic cleft lip with or without cleft palate was shown for single nucleotide polymorphisms in FOXF2 gene in an asian population. *Birth Defects Res A Clin Mol Teratol.* 103(10):857-862.
- Calnan J. 1954. Submucous cleft palate. *Br J Plast Surg.* 69(4):264-282.
- Carlsson P, Mahlapuu M. 2002. Forkhead transcription factors: key players in development and metabolism. *Dev Biol.* 250(1):1-23.
- Clevidence DE, Overdier DG, Peterson RS, Porcella A, Ye H, Paulson KE, Costa RH. 1994. Members of the hnf-3/forkhead family of transcription factors exhibit

- distinct cellular expression patterns in lung and regulate the surfactant protein B promoter. *Dev Biol.* 166(1):195-209.
- De Blacam C, Smith S, Orr D. 2018. Surgery for velopharyngeal dysfunction: a systematic review of interventions and outcomes. *Cleft Palate Craniofac J.* 55(3):405-422.
- Firth HV, Richards SM, Bevan AP, Clayton S, Corpas M, Rajan D, Van Vooren S, Moreau Y, Pettett RM, Carter NP. 2009. Decipher: database of chromosomal imbalance and phenotype in humans using Ensembl resources. *Am J Hum Genet.* 84(4):524-533.
- Gould DB, Mears AJ, Pearce WG, Walter MA. 1997. Autosomal dominant Axenfeld-Rieger anomaly maps to 6p25. *Am J Hum Genet.* 61(3):765-768.
- Harville EW, Wilcox AJ, Lie RT, Vindenes H, Abyholm F. 2005. Cleft lip and palate versus cleft lip only: are they distinct defects? *Am J Epidemiol.* 162(5):448-453.
- Hellqvist M, Mahlapuu M, Blixt A, Enerback S, Carlsson P. 1998. The human forkhead protein FREAC-2 contains two functionally redundant activation domains and interacts with TBP and TFIB. *J Biol Chem.* 273(36):23335-23343.
- Hellqvist M, Mahlapuu M, Samuelsson L, Enerback S, Carlsson P. 1996. Differential activation of lung-specific genes by two forkhead proteins, FREAC-1 and FREAC-2. *J Biol Chem.* 271(8):4482-4490.
- Ishida M, Cullup T, Boustred C, James C, Docker J, English C, GOSgene, Lench N, Copp AJ, Moore GE, et al. 2018. A targeted sequencing panel identifies rare damaging variants in multiple genes in the cranial neural tube defect, anencephaly. *Clin Genet.* 93(4):870-879.

Kaplan EN. 1975. The occult submucous cleft palate. *Cleft palate J.* 12(1):356-368.

Lehmann OJ, Ebenezer ND, Jordan T, Fox M, Ocaka L, Payne A, Leroy BP, Clark BJ, Hitchings RA, Povey S, et al. 2000. Chromosomal duplication involving the forkhead transcription factor gene FOXC1 causes iris hypoplasia and glaucoma. *Am J Hum Genet.* 67(5):1129-1135.

Lupianez DG, Spielmann M, Mundalos S. 2016. Breaking TADs: How alterations of chromatin domains result in disease. *TIG* 32(4):225-237.

Mardini S, Chim H, Seselgyte R, Chen PK. 2016. Predictors of success in furlow palatoplasty for submucous clefts: an experience with 91 consecutive patients. *Plast Reconstr Surg.* 137(1):135e-141e.

McGrath KE, Koniski AD, Maltby KM, McGann JK, Palis J. 1999. Embryonic expression and function of the chemokine SDF-1 and its receptor, CXCR4. *Dev Biol.* 213(2):442-456.

Meskin IH, Gorlin RJ, Isaacson RJ. 1964. Abnormal morphology of the soft palate. I. The prevalence of cleft uvula. *Cleft Palate J.* 35(1):342-346.

Miura N, Kakinuma H, Sato M, Aiba N, Terada K, Sugiyama T. 1998. Mouse forkhead (winged helix) gene Lun encodes a transactivator that acts in the lung. *Genomics.* 50(3):346-356.

Mossey PA, Little J, Munger RG, Dixon MJ, Shaw WC. 2009. Cleft lip and palate. *Lancet.* 374(9703):1773-1785.

Nik AM, Johansson JA, Ghiami M, Reyahi A, Carlsson P. 2016. Foxf2 is required for secondary palate development and Tgfbeta signaling in palatal shelf mesenchyme. *Dev Biol.* 415(1):14-23.

- Ormestad M, Astorga J, Carlsson P. 2004. Differences in the embryonic expression patterns of mouse *Foxf1* and -2 match their distinct mutant phenotypes. *Dev Dyn.* 229(2):328-333.
- Pauws E, Hoshino A, Bentley L, Prajapati S, Keller C, Hammond P, Martinez-Barbera JP, Moore GE, Stanier P. 2009. *Tbx22* null mice have a submucous cleft palate due to reduced palatal bone formation and also display ankyloglossia and choanal atresia phenotypes. *Hum Mol Genet.* 19(15):4171-4179.
- Perry JL. 2011. Anatomy and physiology of the velopharyngeal mechanism. *Semin Speech Lang.* 32(2):83-92.
- Pierrou S, Hellqvist M, Samuelsson L, Enerback S, Carlsson P. 1994. Cloning and characterization of seven human forkhead proteins: binding site specificity and dna bending. *EMBO J.* 13(20):5002-5012.
- Sell D, Harding A, Grunwell P. 1999. Gos.Sp.Ass.'98: an assessment for speech disorders associated with cleft palate and/or velopharyngeal dysfunction (revised). *Int J Lang Commun Disord.* 34(1):17-33.
- Seto-Salvia N, Stanier P. 2014. Genetics of cleft lip and/or cleft palate: association with other common anomalies. *Eur J Med Genet.* 57(8):381-393.
- Sommerlad BC, Fenn C, Harland K, Sell D, Birch MJ, Dave R, Lees M, Barnett A. 2004. Submucous cleft palate: a grading system and review of 40 consecutive submucous cleft palate repairs. *Cleft Palate Craniofac J.* 41(2):114-123.
- Stanier P, Moore GE. 2004. Genetics of cleft lip and palate: syndromic genes contribute to the incidence of non-syndromic clefts. *Hum Mol Genet,* 13 (spec no 1):r73-81.

- Swanson, JW, Mitchell BT, Cohen M, Solot C, Jackson O, Low D, Bartlett SP, Taylor JA. 2017. The effect of furlow palatoplasty timing on speech outcomes in submucous cleft palate. *Ann Plast Surg.* 79(2):156-161.
- Thieme F, Ludwig KU. 2017. The role of noncoding genetic variation in isolated orofacial clefts. *J Dent Res.* 96(11):1238-1247.
- Wang T, Tamakoshi T, Uezato T, Shu F, Kanzaki-Kato N, Fu Y, Koseki H, Yoshida N, Sugiyama T, Miura N. 2003. Forkhead transcription factor Foxf2 (Lun)-deficient mice exhibit abnormal development of secondary palate. *Dev Biol.* 259(1):83-94.
- Xu J, Liu H, Lan Y, Aronow BJ, Kalinichenko VV, Jiang R. 2016. A Shh-Foxf-Fgf18-Shh molecular circuit regulating palate development *PLOS Genet.* 12(1):e1005769.

Figures legends

Figure 1. Egyptian family with absent uvula. A) Absent uvula palate in the proband (IV.5). Note the short posterior border of the soft palate where the uvula should be and unusual structure of the pillar of fauces. SP – Soft palate; ATP – Anterior tonsillar pillar; T – Tonsil. B) Family pedigree showing autosomal dominant inheritance of hypernasality and absent uvula. Eleven family members were genotyped for linkage analysis (+). Exome sequencing analysis was performed on 3 individuals (‡) and Sanger sequencing (*) was used to assess segregation of candidate gene variants in additional individuals (↑).

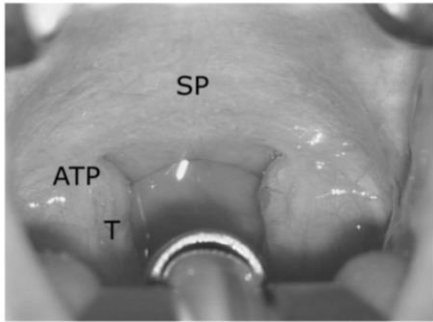
Figure 2. Schematic diagram showing the functional domains of *FOXF2*. A) The location of nonsynonymous missense variants p.A25G, p.A41S and p.Q433P are given. Note that the two N-terminal variants p.A25G, p.A41S were classified bioinformatically as benign. B) The evolutionary conservation of each variant is indicated in the respective boxed areas.

Figure 3. Functional analysis of the *FOXF2* p.Q433P variant. A) Transcriptional activation of *FOXF2* WT and Q433P constructs in HeLa cells. Data represent the average \pm standard deviation of triplicate samples at 24 hours post transfection. B) Quantitative expression difference between the WT and p.Q433P mutation constructs measured by RTqPCR in HeLa cells. C) Western blot showing *FOXF2* protein expression in HeLa cells transfected with *FOXF2* WT, Q433P mutation and pCMV6-XL

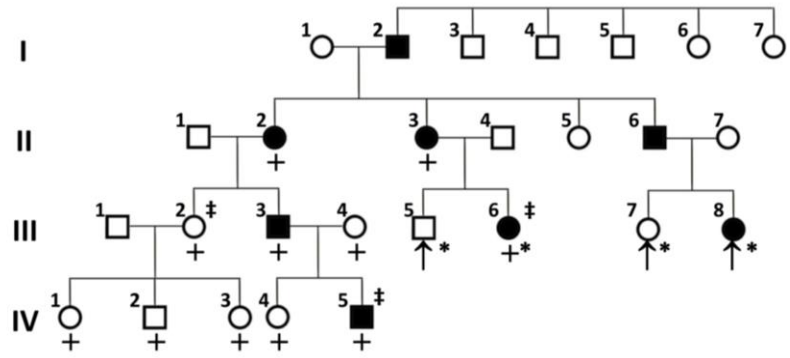
'empty' vector constructs. D) Transcriptional activity normalized to protein level. E) *FGF18* and F) *SHOX2* transcript levels assessed by RTqPCR and normalized to B-Actin in HeLa cells at 24hours following transfection of WT, Q433P constructs and empty vector. All data presented were representative of at least 3 replicate experiments. (** $p < 0.01$; * $p < 0.05$).

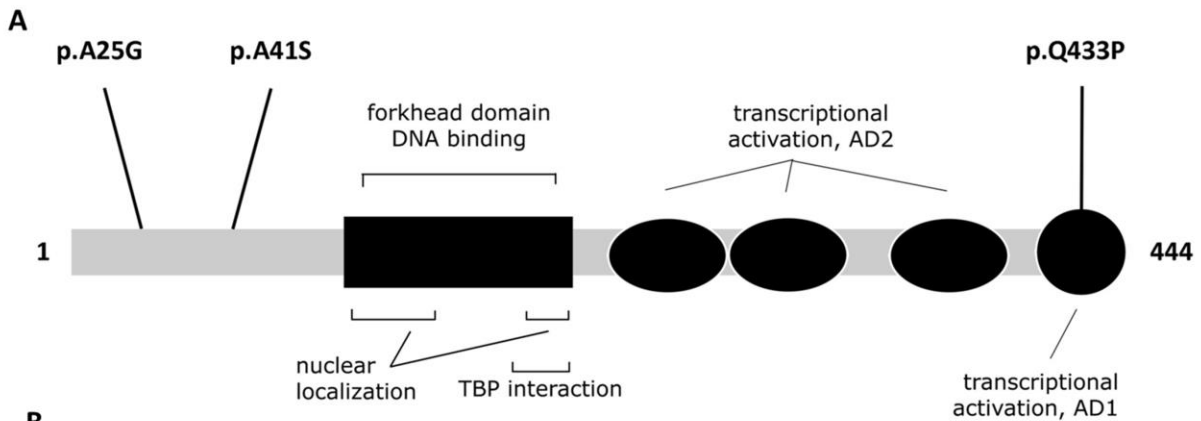
Figure 4. Expression of *FOXF2* in the oral cavity of human embryos. Coronal sections of anterior to posterior (left to right) of human embryo heads at CS22, CS23 and L8pcw (top, middle and bottom panels respectively), showing maxilla, tongue and palatal shelves. The second column is approximately mid palate, the third column is towards the back of the palatal shelves and the fourth column is from among the last sections in each embryo that show the rudimentary palatal shelves (arrow heads) which on fusion will become the uvula. Expression of *FOXF2* is seen in the tongue and also in the palatal shelves. In the developing palate, expression is mostly on the oral half of anterior regions, but becomes more widely expressed throughout the posterior palatal shelf mesenchyme and bordering oral tissues. At later stages, expression includes the more posterior oral epithelial surfaces. (PS - palatal shelf; NS – nasal septum; T – tongue; ES – epithelial seam).

A



B





B

	p.A25G	p.A41S		p.Q433P
Human	ALQAAALMS...AAAAA	PETT.....	HHHQSVCQDIKPCVM	
Rhesus	NNNNNNNNN...NNNNNNNNN		HHHQSVCQDIKPCVM	
Mouse	ALQAAALMS...---	LEST.....	HHHQSVCQDIKPCV	
Dog	ALQAAALRS...---	SAALETN.....	HHHQSVCQDIKPCV	
Elephant	ALQAAALMS...---	ALESA.....	HHHQSVCQDIKPCV	
Chicken	AL----MS...---	ALE--.....	HH----QDIKPCV	
Xenopus	TLOSALMS...---		HHHQSVCQDIKPCV	
Zebrafish	-----...---		HQH-GVCQDVKPCV	

